WARSAW UNIVERSITY OF TECHNOLOGY Index 351733
FACULTY OF CIVIL ENGINEERING
COMMITTEE FOR CIVIL AND WATER ENGINEERING
POLISH ACADEMY OF SCIENCES ISSN 1230-2945

DOI: 10.24425/ace.2022.141901

ARCHIVES OF CIVIL ENGINEERING

Vol. LXVIII ISSUE 3 2022

pp. 539 –551

Research paper

Drying shrinkage and creep properties of self-compacting concrete with expansive agent and viscosity modified admixture

He Liu[1], Guangchao Duan[2], Jingyi Zhang[3]

Abstract: Self-Compacting Concrete (SCC) has been widely used in the filling layer of high-speed railways. The quality of the filling layer directly affects the durability, comfort, and safety of the track system. In this study, shrinkage characteristics and the creep behavior of SCC were investigated by compressive creep tests and shrinkage tests. They were performed on specimens with different loading levels with a calcium sulfoaluminate-based expansive agent (UEA) and viscosity modified admixture (VMA). Furthermore, based on the scanning electron microscope (SEM) morphology of hydration products and X-ray diffraction (XRD) analysis, the influence of admixtures on microstructure and mineral phases of SCC was analyzed.The results show that when concretes were loaded with the same stress level, the main factor influencing creep of SCC was the quantity and microstructure of amorphism and hydration crystal. The XRD and SEM result showed that UEA and VMA make the creep and shrinkage of SCC reduce obviously as the cementitious system grow many crystals in hydration products. The creep of NC was less than SCC with identical compressive strength. At the same time, the addition of UEA can improve the ability to resist drying shrinkage.

Keywords: self-compacting concrete, UEA expansive agent, viscosity modified admixture, creep, drying shrinkage

[1]PhD., Eng., Shenyang Jianzhu University, School of Transportation and Geometics Engineering, No. 25 Hunnan Zhong Road, Hunnan District, 110168 Shenyang, China, e-mail: heliu@sjzu.edu.cn, ORCID: 0000-0002-3867-0726

[2]M.Eng., Shenyang Jianzhu University, School of Transportation and Geometics Engineering, No. 25 Hunnan Zhong Road, Hunnan District, 110168 Shenyang, China, e-mail: d1045339052@163.com, ORCID: 0000-0002-6195-4065

[3]M. Eng., Shenyang Urban Construction University, School of Civil engineering, No.380 Bai Ta Road, Hunnan District, 110167 Shenyang, China, e-mail: dq_zjy@syucu.edu.cn, ORCID: 0000-0003-4641-5191

1. Introduction

The self-compacting concrete (SCC) is a kind of high-performance concrete, which has been presented as an evolutionary technology for a large diversity of applications [1–5]. It has been discovered that SCC has excellent workability that can flow around reinforcement and consolidate under its self-weight without any vibration and has been applied to the CRTS (China Railway Track System) III type slab ballastless track structure [6, 7].

The structure of CRTS III slab ballastless track is shown in Fig. 1, It can be observed that the track ballastless structure consists of four layers, including concrete bottom, geotextile sheet, filling layer, and track slab. Geotextile sheet is manufactured by synthetic fiber, its main function includes insulating SCC filling layer and concrete bottom; decreasing the stress amplitudes caused by temperature gradient stress and further avoiding fracture in SCC filling layer-concrete bottom interface. Furthermore, the geotextile sheet can be replaced with a damping layer when surrounding buildings require low ambient vibration and ambient noise. The damping layer is mainly composed of natural rubber, it has a similar effect as geotextile sheet and can also improve the energy absorption characteristics of CRTS III slab ballastless track [8, 9]. The filling layer is cast-in-place and is required to have strong bonding with the prefabricated track slab. However, creep and shrinkage of SCC for filling layer leads to filling layer deformation and then cause gaps between the prefabricated track slab and the SCC filling layer. Therefore, the creep and shrinkage properties of SCC for filling layer should be carefully designed and researched.

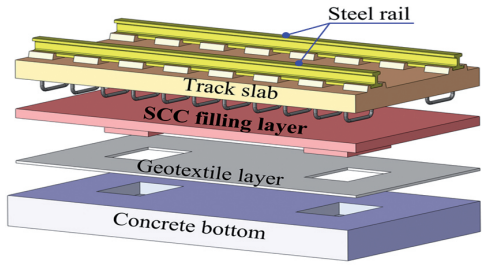

Fig. 1. The structure section and layout of CRTS III slab ballastless track [10]

To meet the high fluidity and high construction efficiency of SCC, it contains a higher paste volume than common concrete. As a result, the shrinkage of SCC is increased due to the excessive use of cement paste [9–11]. The interfacial transition zone between filling layer and track slab is likely to be very weak when the shrinkage of SCC is larger. Fly ash (FA), ground granulated blast furnace slag (GGBS), silica fume (SF) has been used as a replacement for cement [12–14]. Current results indicate that the addition of FA and GGBS decreases drying shrinkage, while the addition of SF results in increased shrinkage [14]. Researchers also suggested that SCC exhibited higher creep than the NC corresponding mixtures. Among these researches, the use of limestone powder may increase creep strain [9], while the use of slag or fly ash appears to decrease the creep strain [15, 16].

Filling layer is a narrow and sealed space with an area of about 14m^2 and thickness of 90mm. Surface of filling layer can't be smoothed by the process of finishing. For that reason, the stability of SCC must be excellent. The effective method is that viscosity modified admixture (VMA) was added in SCC. At the same time, according to the design theory, it is required that excellent bonding strength between filling layer and track plate. Therefore, a larger shrinkage of SCC is acceptable. In order to improve the shrinkage property of SCC, a calcium sulfoaluminate-based expansive agent (UEA) is used to meet the requirements of SCC for filling layer. Influence of VMA and UEA on the properties of concrete was revealed by many researchers. It has been found that stability of entrained air in SCC was improved by VMA [17]. Static stability of SCC was enhanced by VMA [18]. VMA could enhance compressive strength, toughness and fracture properties of SCC [13]. UEA, fiber and the curing conditions are proved efficiently for declining the influences of shrinkage [19–21]. These studies reported a higher final expansion as the UEA additive contents increased.

However, there are no systematic studies about the effects of VMA and UEA on the shrinkage and creep of SCC. This study discussed the effects of UEA and VMA addition on Shrinkage and creep of SCC. Shrinkage and creep properties of NC and SCC at same compressive strength grade were researched. The mechanism of admixture on creep and shrinkage of SCC were analyzed by SEM and XRD. These results could help further to comprehend shrinkage and creep of SCC with UEA and VMA.

2. Methods

2.1. Materials and specimen preparation

The cementitious materials used in the experiment were P.O 42.5 cement complying with Chinese Standard GB175-2007 [24], fly ash (FA), and S95 ground granulated blast furnace slag (GGBS), whose chemical components and specific surface area are shown in Table 1. The VMA is composed of polymer, inorganic ultrafine calcareous, and siliceous powder, and its apparent density was 2.30 g/cm^3. UEA was used to make the mixture attain a certain expansion with an apparent density of 2.80 g/cm^3. Polycarboxylic acid

Table 1. Physical properties and chemical composition of C, FA, GGBS, SF, LP, (by wt%)

Type	SiO_2	Al_2O_3	Fe_2O_3	CaO	MgO	SO_3	eq-Na_2O	Los on ignition (%)	Specific surface area (m^2/kg)	Apparent density (g/cm^3)
C	24.6	7.30	4.00	59.7	3.8	2.5	0.60	2.50	350	3.12
FA	52.3	26.3	9.70	3.70	1.20	1.20	1.80	4.70	450	2.45
GGBS	26.1	13.8	14.1	33.6	8.10	–	0.45	2.10	420	2.78

superplasticizer (SP) with a 30% water-reducing rate was used to achieve good workability of the fresh mixture. The aggregates consisted of river sand (S) with a fineness modulus of 2.48 and with an apparent density of 2.65 g/cm^3, crash aggregate (G) with a maximum particle size of 16 mm. The crash aggregate is supplied by crushed limestone, and its apparent density was 2.70 g/cm^3. The gradation curve of coarse aggregates is shown in Fig. 2.

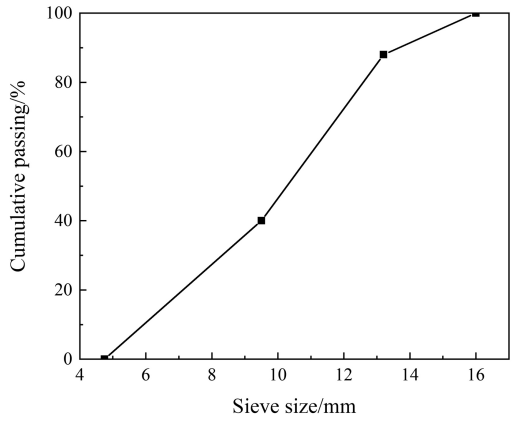

Fig. 2. Gradation curves of coarse aggregate

To research shrinkage and creep properties of NC and SCC with UEA and VMA, an experimental program was launched, in which cubic compressive strength of NC and SCC is C40 grade at 28-day age. Concrete mixing proportions are shown in Table 2. Cementitious materials of SCC–SCC3 are 520 kg/m^3. Contents of FA and GGBS of SCC–SCC3 are 15% and 20% by weight replacement. UEA content of SCC2 is 8% by weight replacement. VMA content of SCC3 is 6% by weight replacement. The water-to-cement ratio (w/c) of SCC and NC was 0.34 and 0.37, respectively. The samples were prepared and tested according to the Chinese standard GB/T50082-2009 [25]. The samples of $100 \times 100 \times 100$ mm^3 and $100 \times 100 \times 400$ mm^3 were demoulded and then cured in corresponding standard experimental conditions $20 \pm 2°$ temperature and more than 95% relative humidity before testing. The expansion value (24 h), compressive strength and modulus of samples are shown in Table 3.

Table 2. Mix proportioning of samples kg/m^3

Code	C	FA	GGBS	UEA	VMA	W	SP	S	G 5–10	G 10–20
SCC1	338	78	104	0	0	178	6.3	835	324	486
SCC2	296	78	104	42	0	178	6.3	835	324	486
SCC3	266	78	104	42	30	178	6.3	835	324	486
NC	292	68	90	0	0	169	2.7	720	420	630

Table 3. Results for expansion value, compressive strength and static elastic modulus

No.	Expansion value/ %	Compressive strength/ MPa	Static elastic modulus/ GPa
SCC1	–	49.2	31.6
SCC2	0.41	51.3	32.8
SCC3	0.43	52.8	33.1
NC	–	54.1	35.8

2.2. Test set up and testing procedure

According to JGJ/T283-2012 [26], slump, slump flow, and concrete stability were measured within 10 min after concrete production and were measured by slump cone. As shown in Table 4, NC and SCC were stable and showed no segregation. Specimens were cast immediately after concrete production and moved to a standard moisture curing chamber. After 24 h, the samples were demolded.

Table 4. Workability of fresh mixture

No.	Slump / mm	T500 / s	Slump flow / mm	Stability
SCC1	255	4.8	670	Good
SCC2	265	5.9	680	Good
SCC3	250	6.2	630	Excellent
NC	153	–	410	Good

The effect of different admixtures on dry-shrinkage properties was analyzed through the dry-shrinkage test. As shown in Fig. 3, after 28-days curing, the specimens were removed from the concrete standard curing room and their lengths were tested as the initial lengths. After this, samples were measured length regularly and repeated three times per measurement. Subsequently, specimen shrinkage was calculated according to Eq. (2.1):

$$\varepsilon_{st} = \frac{L_0 - L_t}{L_b} \tag{2.1}$$

where ε_{st} is the shrinkage of concrete at t days; L_0 is the initial length of the specimen, L_t is the specimen length at t days; L_b is measuring scale distance.

According to GB/T50082-2009 [23], samples for creep tests were cured under standard conditions for 28 days. As shown in Fig. 4, the specimens were put on the measuring systems under a fixed load. In this study, the relationship between creep and different admixtures was measured under corresponded to 40% of the compressive strength of the specific concrete mixtures. The relationship between the creep character and load level was measured under the load corresponded to 30%, 40%, and 50% of the compressive strength of NC and SCC concrete mixtures. After that, the deformation value of samples was tested

at regular times and was calculated according to Eq. (2.2):

$$\varepsilon_{ct} = \frac{\Delta L_t - \Delta L_0}{L_b} - \varepsilon_{st} \tag{2.2}$$

where ε_{ct} is the creep of concrete at t days; ΔL_t is the deformation value of the specimen at t days; ΔL_0 is the Initial deformation value; L_b is measuring scale distance.

Fig. 3. Photograph of the drying shrinkage test

Fig. 4. Photograph of the creep test

Three samples of each type concrete were measured in shrinkage and creep test. The average value of three samples was used as the final test result.

To further analyze the creep mechanism of SCC1~SCC3, the microstructure and hydration product of SCC were analyzed by scanning electron microscopy (SEM) and X-ray diffraction (XRD), as shown in Fig. 5 and Fig. 6. A piece of the sample of each SCC was measured by SEM for microstructure analysis. Capture images at 10000× for the SEM were performed using QUANTA FEG-250 SEM equipment at an accelerating voltage of 20 kV, as shown in Fig. 5. The samples were ground into fine powder to be used for XRD. The 2θ values ranged from 5° and 65°, with an increment of 0.0167° and a measuring time of 59.69 s/ste. Fitting – analysis of all XRD patterns was performed using Highscore plus software.

3. Results and discussion

3.1. Shrinkage of scc with different admixtures

The results for drying shrinkage for each sample are shown in Fig. 5. It can be observed that the early shrinkage rate of SCC is faster than that of NC. From the results given in Fig. 5, the drying shrinkage value of SCC1 is 277 $\mu\varepsilon$. Compared with SCC1, the value of shrinkage in SCC2, incorporating UEA, and in SCC3, with UEA and VMA, are decreased 9.6 and 18%, respectively. The reason for that ettringite crystals was formed by UEA [27]

and cement was replaced by VMA. Additionally, SCC1 showed higher final values of drying shrinkage than NC. The lower drying shrinkage of NC compared to SCC1 is caused by the different amounts of paste volume. As shown in Fig. 5, SCC3 offers the benefit of low drying shrinkage. The results showed that the incorporation of UEA and VMA could effectively mitigate the drying shrinkage deformation.

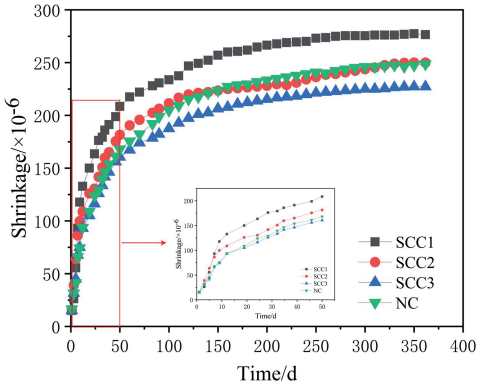

Fig. 5. The variation of drying shrinkage of SCC samples with testing age

3.2. Creep of scc with different admixtures

The creep strain curves are shown in Fig. 6. The creep strain curves have the following three stages: rapid development, transition, and stability. The creep strains rapidly increased for all samples, and these rates were essentially identical at the initial stage. Creep strain values of the SCC sample slightly exceeded that of the NC samples at a loading age of 28 d. And the final creep value of SCC1 is larger than that of the NC sample with the same

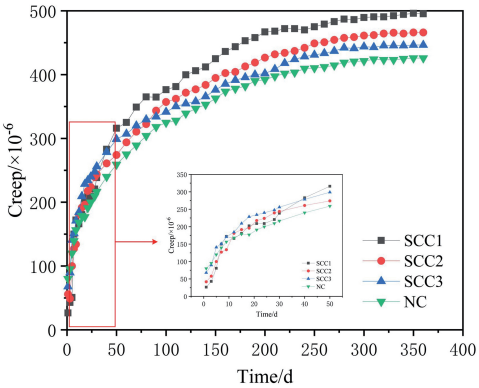

Fig. 6. The creep vs testing age curves of SCC samples by loading 40% peak stress

strength grade. The value of SCC1 tested is basically in accordance with results reported by researchers [28,29]. Compared with SCC1, the absolute creep value in SCC2 and SCC3 decreased 5.9% and 9.8%, respectively. The creep of SCC3 is slightly higher than NC with the same strength grade, and this suggested that the addition of UEA and VMA could effectively mitigate the creep deformation of SCC. The coarse aggregate content in NC differs from SCC, which is 660 L/m^3 and 615 L/m^3, respectively. The rocks have higher elasticity modulus and strength, higher content of rock cause a lower creep.

The relationship between the creep character and load level is shown in Fig. 7. The loads corresponded to 30%, 40%, and 50% of the compressive strength of the specific concrete mixtures, respectively. The creep of normal concrete with the same strength grade (C40) was also tested for comparison purposes. Fig. 7 indicated that the creep of SCC is higher than that of NC with different load levels. Furthermore, SCC3 marked a significant increase in creep value when the load level was at 50% of the ultimate load.

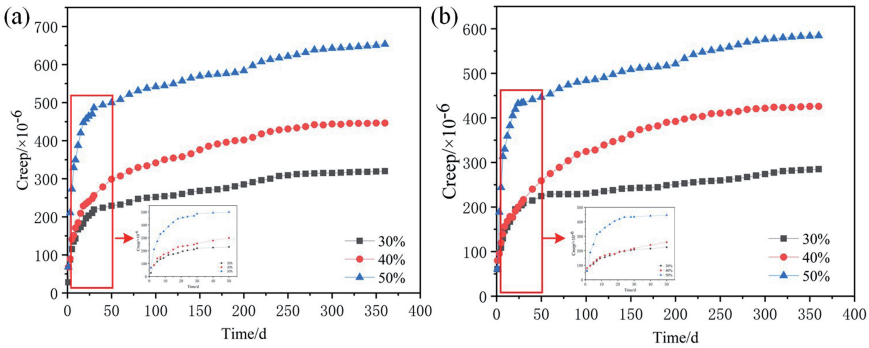

Fig. 7. Creep value of samples under different load levels: a) SCC3, b) NC

The isochronous stress-strain curve was used to analyze the creep characteristics of SCC and NC based on the contrast of loads. Isochronous stress-strain curves are the relationship curves of creep deformation and stress simultaneously among a cluster of creep curves on different stress levels. An isochronous curve in the stress-strain coordinate is drawn by each intersection's stress-strain value, obtained by drawing a straight line that parallels the longitudinal axis on Fig. 7 and intersects with the creep curves on different load levels.

As shown in Fig. 8, the isochronous stress-strain curves of SCC3 and NC trend towards the X-axis gradually with the increase of stress and time. When the stress is low, the spacing of isochronous stress-strain curves is small. With the rise of stress, the spacing of curves gradually increases, which indicates that the creep of SCC3 and NC has an obvious non-linear characteristic. With the increase of stress, the time effect of stress-strain in the creep process gradually increases. Meanwhile, the isochronous stress-strain curves of SCC3 trend more towards the X-axis with the increase of load level, the slope of SCC3 is less than that of NC in turning points, which is contributed by a high volume of cement paste in the SCC3 sample. The results show that the deformation capacity of SCC3 is more sensitive to load compared with NC.

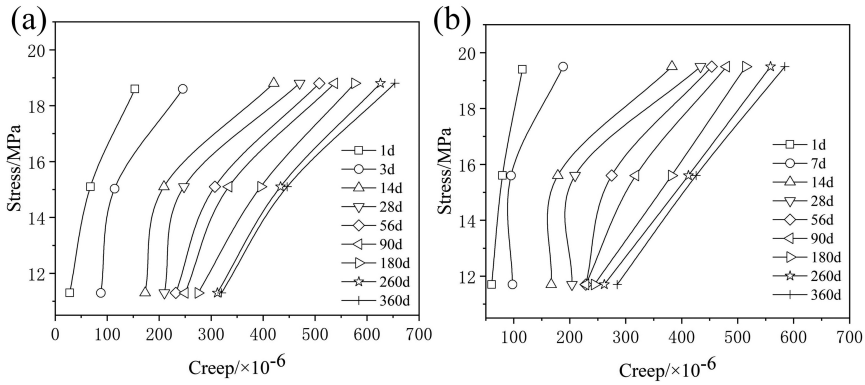

Fig. 8. Isochronic stress-strain relationship of the samples: a) SCC3, b) NC

3.3. Mechanism analyze

Compared with SCC, the creep value of NC is lower. It is due to the aggregate volume of NC being 66.0% of total concrete volume, which is higher than that in SCC (61.5% of total concrete volume). Aggregate is inert materials. The deformation of aggregate under load is little and possible to ignore, which results in a lower creep value of NC.

To further explore the creep mechanism of SCC1–SCC3, unhydrated cement particles, and crystals in hydration products were assumed to be inert material. The amorphous phase was supposed to be flow and deformation under load. When the concretes were loaded with equivalent stress levels, the main effect of influencing the creep characteristics of concrete is the quantity of amorphous phase [30, 31]. XRD analysis results are presented in Fig. 9 and Fig. 10. The amorphous phase and hydration crystal phase were the main hydration products of the cementitious phase, in which the amorphous phase could not be identified by XRD. In this study, the amorphous phase is the calculation of the difference between all the phases and hydration crystal phases. As shown in Fig. 9, the main products of each sample were quartz (Qu), mullite (Mu), C_4AF, Ettringite (Ett), monocarbone (Mc), calcite (Cc), portlandite (CH), hemicarboaluminate (Hc), C_3S, and C_2S. Fig. 10 indicates that amorphous phase contents of SCC1 – SCC3 are 46.37%, 39.64% and 35.35%, respectively. Ett contents of SCC1 – SCC3 are 0%, 5.8% and 7.89%, respectively. The main reason may be that C is replaced by UEA and VMA which leads to content of Ca^{2+} ion decrease. Ca^{2+} ion is important component of amorphous phase (C–S–H) which affects the formation of amorphous phase content. Al^{3+} content is increasing when amorphous phase (C–S–H) is decreasing. With Al^{3+} content increasing which can promote Ett phase formation. Due to total amorphous phase content decreases which leads to less creep value of SCC2 and SCC3.

In order to verify the test results of XRD, the microstructure of SCC with different admixtures was analyzed, as shown in Fig. 11. It can be seen from Fig. 11a that the main hydration product of SCC1 is irregular amorphous. Fig. 11b indicates that in the case of SCC2 modified with UEA, in contrast to SCC1, ettringite (Ett) is present in the sample in

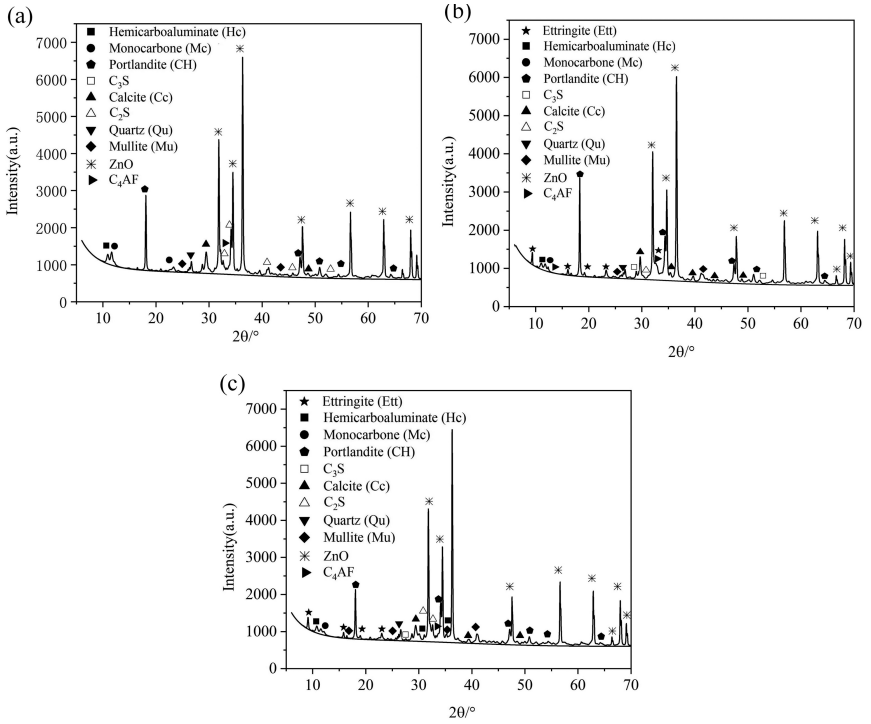

Fig. 9. XRD patterns of the samples with different admixture: a) SCC1, b) SCC2, c) SCC3

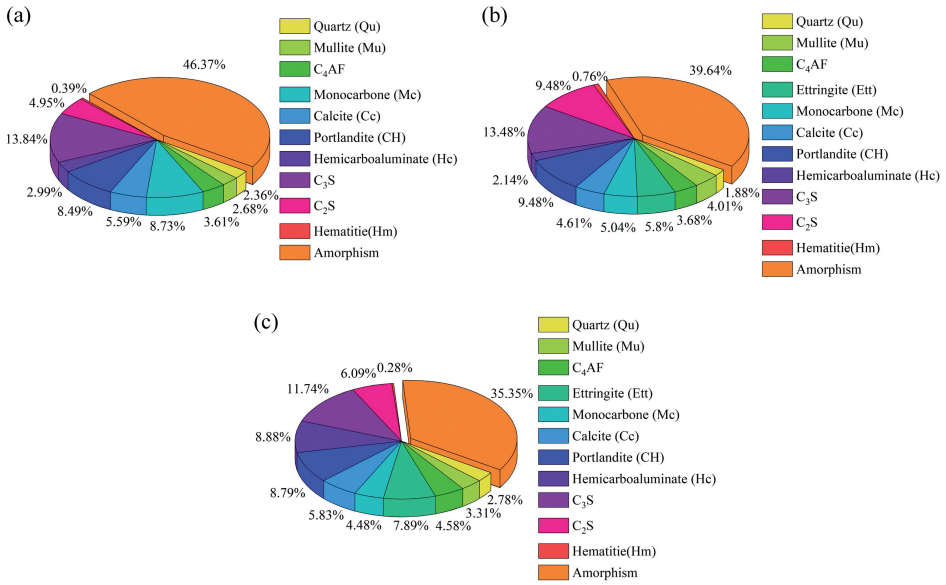

Fig. 10. The mass fraction of each substance: a) SCC1, b) SCC2, c) SCC3

the needle-shaped. Furthermore, SCC2 is characterized by a higher amount of C_3S phase (9.48%) and C_2S phase (13.48%) and thus improving the creep character of SCC2. Fig. 11c indicated that in the case of SCC3, more hydration crystals can be found under SEM. SCC3 shows more Ett, which is bigger in length than SCC2. The SEM results proved the validity of the XRD result, this gives a possible explanation for the lower creep values in SCC3 with UEA and VMA content.

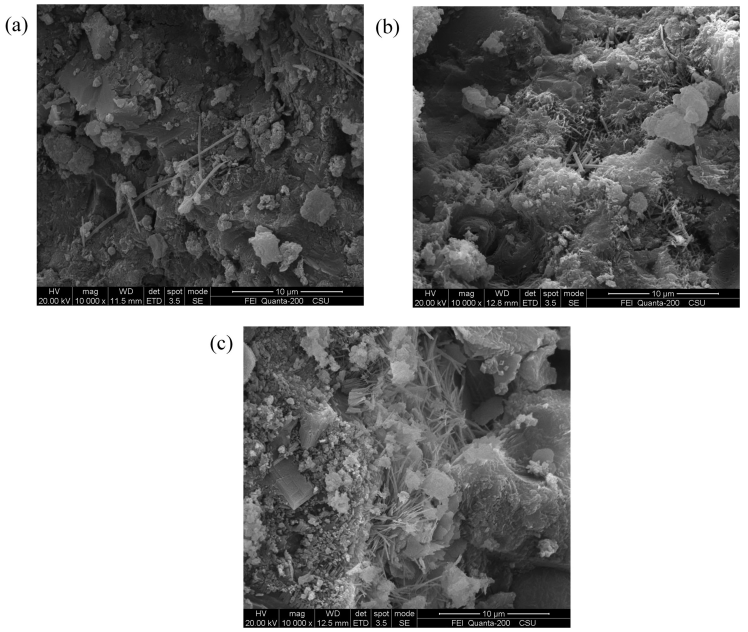

Fig. 11. SEM result of the samples with different admixture: a) SCC1, b) SCC2, c) SCC3

UEA and VMA produced in SCC as indicated by XRD and SEM might have helped to improve creep performance. In this research, SCC shows a decrease in shrinkage and creep with VMA and UEA. This is attributed to VMA and UEA contributing to the increase in ettringite crystal products and decreased amorphous products, which can retard the shrinkage and creep.

4. Conclusions

This paper investigated the effects of UEA and VMA on shrinkage and creep of SCC. Based on the above experimental results, the main conclusions could be summarized as follows:

1. Shrinkage is mainly dominated by the paste volume, compared with NC, SCC has a higher value of paste volume. Besides, compared with SCC1, the shrinkage value of SCC2 and SCC3 are decreased 9.6% and 18%, respectively. The incorporation of UEA and VMA could effectively mitigate the drying shrinkage.

2. Compared with NC, the creep of SCC1 is higher, due to the higher paste volume of paste in the SCC1 mixture. The creep strain of SCC3 is lower than SCC1 and SCC2. The incorporation of UEA and VMA could effectively mitigate the creep strain.
3. The isochronous stress-strain curves of SCC3 and NC indicated that with the increase of stress, the time effect of stress-strain in the creep process gradually increases. Compared with NC, the deformation capacity of SCC3 is more sensitive to load.
4. Based on the results of XRD and SEM, with the combination of UEA and VMA, the hydration products have a trend of crystallizing, resulting in the decrease of the creep of SCC.

Acknowledgements

This work was supported by Doctor Start-up Foundation of Liaoning province (grant numbers 2021-BS-166) and Foundation of Liaoning Province Education Administration (grant numbers lnqn202017).

References

[1] E.G. Badogiannis, I.P. Sfikas, D.V. Voukia, et al., "Durability of metakaolin self-compacting concrete", *Construction and Building Materials*, 2015, vol. 82, pp. 133–141, DOI: 10.1016/j.conbuildmat.2015.02.023.

[2] K. Behfarnia, O. Farshadfar, "The effects of pozzolanic binders and polypropylene fibers on durability of SCC to magnesium sulfate attack", *Construction and Building Materials*, 2013, vol. 38, pp. 64–71, DOI: 10.1016/j.conbuildmat.2012.08.035.

[3] H.J.H. Brouwers, H.J. Radix, "Self-Compacting Concrete: Theoretical and experimental study", *Cement and Concrete Research*, 2005, vol. 35, no. 11, pp. 2116–136, DOI: 10.1016/j.cemconres.2005.06.002.

[4] Q. Cao, Y. Cheng, M. Cao, Q. Gao, "Workability, strength and shrinkage of fiber reinforced expansive self-consolidating concrete", *Construction and Building Materials*, 2017, vol. 131, pp. 178–185, DOI: 10.1016/j.conbuildmat.2016.11.076.

[5] P. Carballosa, J.L.G. Calvo, D. Revuelta, et al., "Influence of cement and expansive additive types in the performance of self-stressing and self-compacting concretes for structural elements", *Construction and Building Materials*, 2015, vol. 93, pp. 223–229, DOI: 10.1016/j.conbuildmat.2015.05.113.

[6] B. Craeye, G. De Schutter, B. Desmet, et al., "Effect of mineral filler type on autogenous shrinkage of self-compacting concrete", *Cement and Concrete Research*, 2010, vol. 40, no. 6, pp. 908–913, DOI: 10.1016/j.cemconres.2010.01.014.

[7] H. Fathi, T. Lameie, M. Maleki, R. Yazdani, "Simultaneous effects of fiber and glass on the mechanical properties of self-compacting concrete", *Construction and Building Materials*, 2017, vol. 133, pp. 443–449, DOI: 10.1016/j.conbuildmat.2016.12.097.

[8] X. Tao, Y. Ding, P. Wang, et al., "Application of rubber mats in transition zone between two different slab tracks in high-speed railway", *Construction and Building Materials*, 2020, vol. 243, art. ID 118219, DOI: 10.1016/j.conbuildmat.2020.118219.

[9] X.W. Sheng, W.Q. Zheng, Z.H. Zhu, et al., "Full-scale fatigue test of unit-plate ballastless track laid on long-span cable-stayed bridge", *Construction and Building Materials*, 2020, vol. 247, art. ID 118601, DOI: 10.1016/j.conbuildmat.2020.118601.

[10] N. Li, G. Long, Q. Fu, et al., "Dynamic mechanical characteristics of filling layer self-compacting concrete under impact loading", *Archives of Civil and Mechanical Engineering*, 2019, vol. 19, no. 3, pp. 851–861, DOI: 10.1016/j.acme.2019.03.007.

[11] M. Gesoğlu, E. Güneyisi, E. Özbay, "Properties of self-compacting concretes made with binary, ternary, and quaternary cementitious blends of fly ash, blast furnace slag, and silica fume", *Construction and Building Materials*, 2009, vol. 23, no. 5, pp. 1847–1854, DOI: 10.1016/j.conbuildmat.2008.09.015.

[12] P. Ghoddousi, A.M. Abbasi, "Influence of aggregate grading and cement paste volume on drying shrinkage of self-consolidating concrete", in *3rd North American conference on the design and use of self-consolidating concrete 2008.* Chicago, 2008.

[13] G. Heirman, L. Vandewalle, D. Van Gemert, et al., "Time-dependent deformations of limestone powder type self-compacting concrete", *Engineering Structures*, 2008, vol. 30, no. 10, pp. 2945–2956, DOI: 10.1016/j.engstruct.2008.04.009.

[14] W. Li, K. Ma, G. Long, et al., "Influence of workability parameters and filling time on the quality of SCC filling layers", *Magazine of Concrete Research*, 2021, vol. 73, no. 12, pp. 636–647, DOI: 10.1680/jmacr.19.00342.

[15] G. Long, H. Liu, K. Ma, et al., "Development of high-performance self-compacting concrete applied as the filling layer of high-speed railway", *Journal of Materials in Civil Engineering*, 2018, vol. 30, no. 2, DOI: 10.1061/(ASCE)MT.1943-5533.0002129.

[16] R. Loser, A. Leemann, "Shrinkage and restrained shrinkage cracking of self-compacting concrete compared to conventionally vibrated concrete", *Materials and Structures*, 2009, vol. 42, no. 1, pp. 71–82, DOI: 10.1617/s11527-008-9367-9.

[17] H. Okamura, M. Ouchi, "Self-compacting high performance concrete", *Structural Engineering and Materials*, 1998, vol. 1, no. 4, pp. 378–383, DOI: 10.1002/pse.2260010406.

[18] A.M. Poppe, G. De Schutter, "Creep and shrinkage of self-compacting concrete", in *First International Symposium on Design, Performance and Use of Self-Consolidating Concrete, 2005*. China, 2005, pp. 329–336.

[19] S. Rath, M. Ouchi, N. Puthipad, et al., "Improving the stability of entrained air in self-compacting concrete by optimizing the mix viscosity and air entraining agent dosage", *Construction and Building Materials*, 2017, vol. 148, no. 1, pp. 531–537, DOI: 10.1016/j.conbuildmat.2017.05.105.

[20] J. Assaad, K.H. Khayat, J. Daczko, "Evaluation of Static Stability of Self-Consolidating Concrete", *Aci Materials Journal*, 2004, vol. 101, no. 3, pp. 168–176.

[21] R.P. Lohtia, B.D. Nautiyal, O.P. Jain, "Creep af Fly Ash Concrete", *Journal Proceedings*, 1976, vol. 73, no. 8, pp. 469–472.

[22] I.G. Richardson, A.R. Brough, G.W. Groves, et al., "The characterization of hardened alkali-activated blast-furnace slag pastes and the nature of the calcium silicate hydrate (C–S–H) phase", *Cement and Concrete Research*, 1994, vol. 24, no. 5, pp. 813–829, DOI: 10.1016/0008-8846(94)90002-7.

[23] E. Rozière, S. Granger, P. Turcry, et al., "Influence of paste volume on shrinkage cracking and fracture properties of self-compacting concrete", *Cement and Concrete Composites*, 2007, vol. 29, no 8, pp. 626–636, DOI: 10.1016/j.cemconcomp.2007.03.010.

[24] *GB175-2007 Common portland cement*. Chinese National Standard, 2007.

[25] *GB/T 50082-2009 Standard for test methods of concrete physical and mechanical properties*. Chinese National Standard, 2009.

[26] *JGJ/T 283-2012 Technical specification for application of self-compacting concrete*. Chinese National Standard, 2012.

[27] S. Nagataki, H. Gomi, "Expansive admixtures (mainly ettringite)", *Cement and Concrete Composites*, 1998, vol. 20, no. 2-3, pp. 163–170, DOI: 10.1016/S0958-9465(97)00064-4.

[28] A. Leemann, P. Lura, R. Loser, "Shrinkage and creep of SCC – The influence of paste volume and binder composition", *Construction and Building Materials*, 2011, vol. 25, no. 5, pp. 2283–2289, DOI: 10.1016/j.conbuildmat.2010.11.019.

[29] M. Vieira, A. Bettencourt, "Deformability of Hardened SCC. Proc", in *3rd Int. RILEM Symp. on SCC*, O. Wallevik, I. Nielsson, Eds. RILEM Publications, S.R.A.L., 2003, pp. 637–644.

[30] Q. Zhao, X. Liu, J. Jiang, "Effect of curing temperature on creep behavior of fly ash concrete", *Construction and Building Materials*, 2015, vol. 96, pp. 326–333, DOI: 10.1016/j.conbuildmat.2015.08.030.

[31] Z. Li, H. Du, Z. Wang, C. Jin, "Experimental Investigation of MgAl-NO2 and MgAl-CO3 LDHs on Durability of Mortar and Concrete", *Advances in Materials Science and Engineering*, 2021, vol. 2021, pp. 1–20, DOI: 10.1155/2021/5582150.

Received: 19.02.2022, Revised: 29.03.2022